AMERICAN SOCIETY FOR MICROBIOLOGY | Journal of Virology®

VIRUS-CELL INTERACTIONS

Varicella-Zoster Virus ORF63 Protects Human Neuronal and Keratinocyte Cell Lines from Apoptosis and Changes Its Localization upon Apoptosis Induction

Chelsea Gerada,[a] Megan Steain,[a] Brian P. McSharry,[a] Barry Slobedman,[a] Allison Abendroth[a]

[a]Discipline of Infectious Diseases and Immunology, The University of Sydney, Camperdown, New South Wales, Australia

ABSTRACT There are many facets of varicella-zoster virus (VZV) pathogenesis that are not fully understood, such as the mechanisms involved in the establishment of lifelong latency, reactivation, and development of serious conditions like postherpetic neuralgia (PHN). Virus-encoded modulation of apoptosis has been suggested to play an important role in these processes. VZV open reading frame 63 (ORF63) has been shown to modulate apoptosis in a cell-type-specific manner, but the impact of ORF63 on cell death pathways has not been examined in isolation in the context of human cells. We sought to elucidate the effect of VZV ORF63 on apoptosis induction in human neuron and keratinocyte cell lines. VZV ORF63 was shown to protect differentiated SH-SY5Y neuronal cells against staurosporine-induced apoptosis. In addition, VZV infection did not induce high levels of apoptosis in the HaCaT human keratinocyte line, highlighting a delay in apoptosis induction. VZV ORF63 was shown to protect HaCaT cells against both staurosporine- and Fas ligand-induced apoptosis. Confocal microscopy was utilized to examine VZV ORF63 localization during apoptosis induction. In VZV infection and ORF63 expression alone, VZV ORF63 became more cytoplasmic, with aggregate formation during apoptosis induction. Taken together, this suggests that VZV ORF63 protects both differentiated SH-SY5Y cells and HaCaT cells from apoptosis induction and may mediate this effect through its localization change during apoptosis. VZV ORF63 is a prominent VZV gene product in both productive and latent infection and thus may play a critical role in VZV pathogenesis by aiding neuron and keratinocyte survival.

IMPORTANCE VZV, a human-specific alphaherpesvirus, causes chicken pox during primary infection and establishes lifelong latency in the dorsal root ganglia (DRG). Reactivation of VZV causes shingles, which is often followed by a prolonged pain syndrome called postherpetic neuralgia. It has been suggested that the ability of the virus to modulate cell death pathways is linked to its ability to establish latency and reactivate. The significance of our research lies in investigating the ability of ORF63, a VZV gene product, to inhibit apoptosis in novel cell types crucial for VZV pathogenesis. This will allow an increased understanding of critical enigmatic components of VZV pathogenesis.

KEYWORDS apoptosis, human herpesviruses, varicella zoster virus

Varicella-zoster virus (VZV) is a human alphaherpesvirus that can cause both varicella (chicken pox) and herpes zoster (shingles). Varicella results from initial VZV infection, where a variety of skin cells, such as keratinocytes, are infected to produce the characteristic varicella rash (1). The nerve endings of sensory neurons dock in the keratinocyte layer of the dermis, allowing the virus to infect sensory neurons and establish lifelong latency in the dorsal root ganglia (DRG) (1). VZV often reactivates later in life to cause herpes zoster, which encompasses a variety of debilitating complica-

Received 6 March 2018 **Accepted** 14 March 2018

Accepted manuscript posted online 28 March 2018

Citation Gerada C, Steain M, McSharry BP, Slobedman B, Abendroth A. 2018. Varicella-zoster virus ORF63 protects human neuronal and keratinocyte cell lines from apoptosis and changes its localization upon apoptosis induction. J Virol 92:e00338-18. https://doi.org/10.1128/JVI.00338-18.

Editor Rozanne M. Sandri-Goldin, University of California, Irvine

Address correspondence to Allison Abendroth, allison.abendroth@sydney.edu.au.

tions, one of the most significant being postherpetic neuralgia (PHN). PHN involves severe neuropathic pain that can last for months or years following the resolution of the herpes zoster rash (2). The mechanisms responsible for VZV's ability to establish latency, reactivate, and cause PHN have not been fully elucidated; however, it has been suggested that the ability of VZV to modulate apoptosis could play a critical role in these processes (3).

Apoptosis is a programmed, noninflammatory form of cell death that is utilized by the intrinsic, innate, and adaptive immune responses to eliminate potentially harmful cells (4). Biochemically, apoptosis can be triggered by two distinct signaling pathways, the extrinsic and intrinsic pathways. The intrinsic pathway is initiated by a diverse range of intracellular stimuli, such as DNA damage and endoplasmic reticulum (ER) stress. These stimuli activate proapoptotic Bcl-2 family members, which causes the oligomerization of Bax with Bak at the mitochondrial membrane (4–7). This results in disruption of the mitochondrial membrane potential and activation of initiator caspases (8). Anti-apoptotic Bcl-2 proteins can bind to proapoptotic Bcl-2 proteins to inhibit this process (9). Thus, the balance of these anti- and proapoptotic Bcl-2 family members is critical in the induction of apoptosis (4, 10). Initiator caspases can cleave effector caspases, such as caspase 3, resulting in morphological apoptotic changes (4, 11). In contrast, the extrinsic pathway is initiated by ligand-induced oligomerization of cell surface receptors, such as Fas, which causes the cleavage of initiator caspases like caspase 8 (12). Caspase 8 can cleave caspase 3, resulting in apoptosis; however, it can also cleave Bid, which can signal through the mitochondria to induce apoptosis (4, 13). Apoptosis is an important host defense mechanism utilized during viral infection to limit viral dissemination. As such, many viruses have evolved to modulate apoptotic pathways (14).

Members of the herpesvirus family have evolved a variety of different mechanisms to manipulate the apoptotic pathway, and this may facilitate viral spread, the maintenance of latency, and successful reactivation (15). Gammaherpesviruses, including Epstein-Barr virus (EBV), encode Bcl-2 homologs to disrupt apoptosis (16). Betaherpesviruses, such as human and murine cytomegalovirus (CMV), interfere with Bax and Bak to inhibit apoptosis, among other mechanisms (17–19). Alphaherpesviruses, such as herpes simplex virus 1 (HSV-1), have been found to inhibit proapoptotic Bcl-2 family members (20) and to regulate prosurvival signaling (21). Interestingly, VZV has been found to modulate apoptosis in a cell-type-specific manner (22). It has been reported that VZV induces apoptosis in skin cell types, such as human fibroblasts (HFs) (22) and MeWo cells (23), and in immune cells, such as T cells, B cells, monocytes (24, 25), and Vero cells (26). In contrast, VZV has been found to protect against apoptosis in human neurons (22, 27). This is thought to be critical to allow VZV to establish lifelong latency in the DRG. Interestingly, the ability of VZV to induce apoptosis in keratinocytes, a critical cell type in VZV pathogenesis, has not been fully characterized.

Several VZV gene products have been associated with the inhibition of apoptosis. Open reading frame 66 (ORF66) has been suggested to inhibit apoptosis in T cells (23, 28), and ORF12 has been shown to trigger extracellular signal-regulated kinase (ERK) phosphorylation to inhibit apoptosis in MeWo cells and human embryonic kidney (HEK293T) cells (29–31). The ORF63 gene is essential for VZV replication and is duplicated within the VZV genome (as ORF70); it is also abundantly transcribed in neuronal latency (32–34). Our laboratory has previously utilized an ORF63 single-knockout virus to determine that ORF63 can inhibit apoptosis in neuronal cells, but not in HFs (27). However, the ability of VZV ORF63 alone to protect against apoptosis has not been examined in the context of human neuronal cells. Furthermore, it is not clear whether this phenotype extends to other clinically relevant cell types, such as keratinocytes. Thus, it is important to elucidate the role of ORF63 in apoptosis in the context of both neuronal and nonneuronal cells due to its importance in latency and reactivation.

We constructed novel VZV ORF63-expressing SH-SY5Y and HaCaT cell lines via a lentivirus expression system to characterize the ability of VZV ORF63 to protect against apoptosis. SH-SY5Y cells are able to undergo intrinsic apoptosis but not extrinsic

apoptosis due to a lack of caspase 8 (35). In this report, we show that VZV ORF63 expression alone can inhibit apoptosis in differentiated human SH-SY5Y neuronal cells, extending our previous work (22, 27). We also establish that this phenotype is not exclusive to neurons, as VZV ORF63 expression alone can also protect a human keratinocyte line (HaCaT cells) from both extrinsic and intrinsic apoptosis. Furthermore, we begin to elucidate how ORF63 mediates its protective effect by showing that VZV ORF63 relocalizes during apoptosis induction in HaCaT cells, implying a potential modulatory function of ORF63 in the cytoplasm of infected cells.

RESULTS

Validation of VZV ORF63-expressing differentiated SH-SY5Y cells. Our laboratory has previously reported that VZV can protect neurons from apoptosis and determined that VZV ORF63 expression alone could protect rat neurons from nerve growth factor (NGF) withdrawal-induced apoptosis (22, 27). However, it is still not known whether VZV ORF63 alone can protect human neuronal cells from apoptosis. We have also previously demonstrated VZV productive infection of the differentiated SH-SY5Y neuroblastoma cell line (36); thus, these cells provide a suitable neuronal model to examine the effects of VZV ORF63 on apoptosis. To investigate this, a hemagglutinin (HA)-tagged VZV ORF63-expressing SH-SY5Y cell line was generated via the construction of a VZV ORF63 pseudovirus and subsequent transduction and selection (Fig. 1A to E). In parallel, an empty control pseudovirus was generated to create control transduced (CT) SH-SY5Y cells. The SH-SY5Y cell line can be differentiated to morphologically and biochemically resemble primary human neurons (37). Previously, we demonstrated that an all-*trans*-retinoic acid (ATRA) and brain-derived neurotrophic factor (BDNF) differentiation protocol causes SH-SY5Y cells to develop extensive neuronal processes and to upregulate markers that are present in primary human neurons, such as synaptophysin and neural cell adhesion molecule (NCAM) (36).

In three biological replicates, SH-SY5Y cells were differentiated using ATRA and BDNF. Both light microscopy images (Fig. 1A) and staining for NCAM by immunofluorescence assay (IFA) (Fig. 1B) showed the development of extensive neuronal processes in the differentiated VZV ORF63, CT, and untransduced (UT) SH-SY5Y cells that were absent from undifferentiated SH-SY5Y cells. Additionally, staining for synaptophysin demonstrated increased synaptophysin expression and localization to neurites when the VZV ORF63, CT, and UT SH-SY5Y cells were differentiated, in contrast to the undifferentiated cells, which demonstrated minimal staining (Fig. 1C). Altogether, this demonstrates that differentiating VZV ORF63, CT, and UT SH-SY5Y cells using an ATRA and BDNF treatment regime yields mature neuronal-like cells that are both morphologically and biochemically similar to primary human neurons. Immunostaining for HA and ORF63 showed that differentiated VZV ORF63 SH-SY5Y cells expressed ORF63 in both the nucleus and cytoplasm, which is consistent with previous findings (Fig. 1D) (38). Flow cytometry staining for intracellular HA revealed that on average 30% of cells were positive after selection and differentiation (Fig. 1E). As expected, no HA-specific staining was observed in control transduced or untransduced differentiated SH-SY5Y cells by either method (Fig. 1B to E).

VZV ORF63 inhibits staurosporine-induced apoptosis in differentiated SH-SY5Y cells. The intrinsic apoptotic pathway was examined in the differentiated SH-SY5Y cells via the use of staurosporine, an inhibitor of protein kinase C (PKC) (39). VZV ORF63, CT, and UT SH-SY5Y cells were differentiated on coverslips using ATRA and BDNF, as previously described (36), and treated with 0.5 μM staurosporine for 4 h. The cells were immunostained for the markers of apoptosis; DNA fragmentation via terminal deoxynucleotidyltransferase-mediated dUTP-biotin nick end labeling (TUNEL) staining and cleaved caspase 3 (CC3), to determine the extent of apoptosis induction (Fig. 2A to C). TUNEL and CC3 staining was readily observed within CT and UT SH-SY5Y cells; however, fewer TUNEL- and CC3-positive cells were seen in the ORF63 SH-SY5Y cells (Fig. 2A to C). To quantitate this difference, 10 independent fields of view for each cell type were enumerated for CC3- and TUNEL-positive cells over three independent

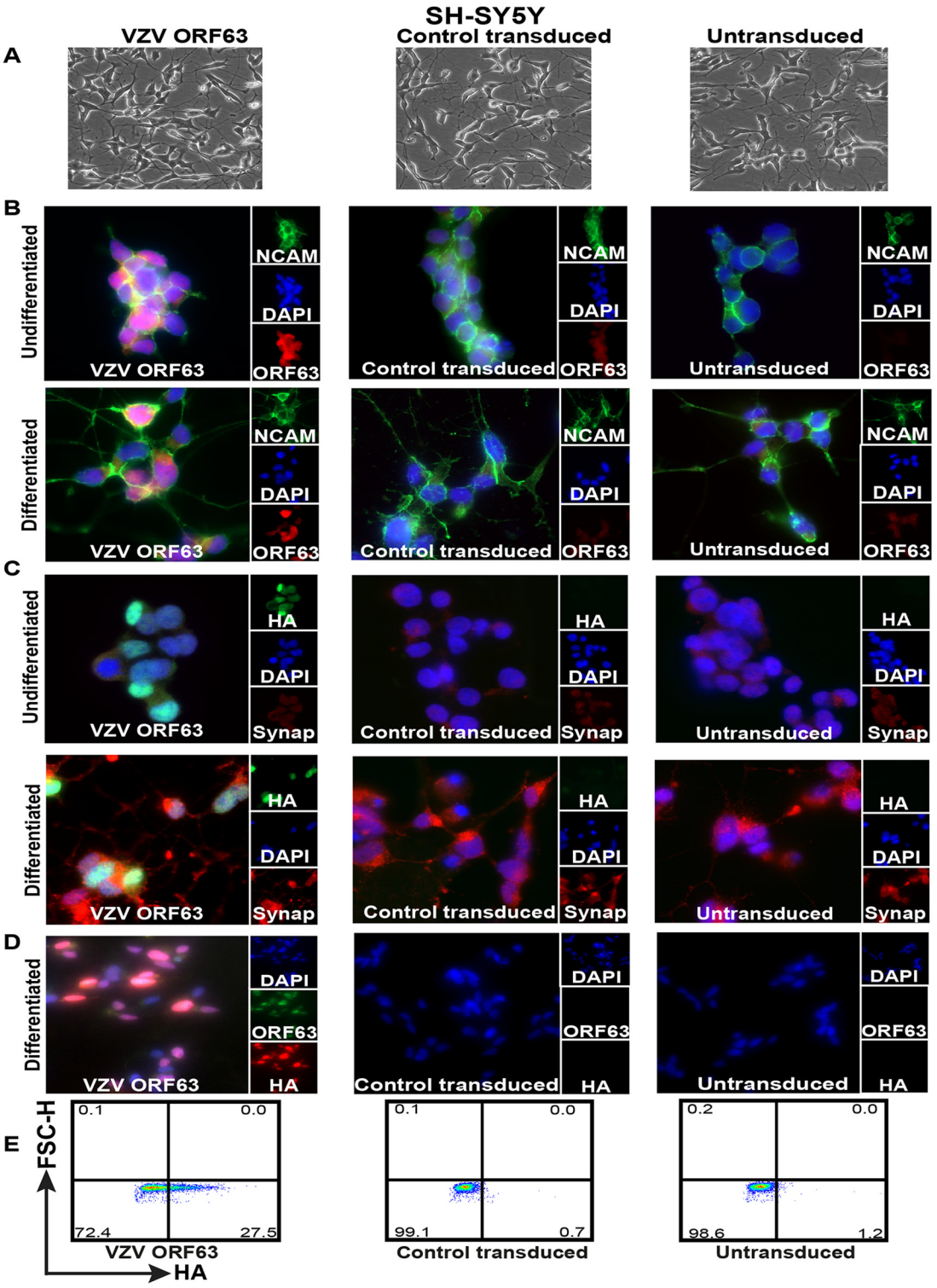

FIG 1 Validation of HA-tagged VZV ORF63-expressing differentiated SH-SY5Y cells. (A) SH-SY5Y cells (1.5×10^6) were transduced with VZV ORF63 or CT pseudoviruses and selected with 0.4 mg/ml G418 for 10 days to create VZV ORF63, CT, and untransduced SH-SY5Y cells. These cells were differentiated using 10 μM ATRA for 5 days and 50 ng/ml BDNF for 4 days. The cells were imaged by light microscopy at the end of the differentiation protocol; the images are shown at $\times$20 magnification. (B to D) VZV ORF63, control transduced, and untransduced SH-SY5Y cells (1×10^5) were differentiated on Matrigel-coated coverslips (13 mm; Knittel glass), fixed with 4% PFA, and stained for VZV ORF63 and NCAM (B), HA and synaptophysin (C), or VZV ORF63 and HA (D). The cells were counterstained with nuclear DAPI (blue) and were visualized by fluorescence microscopy. The images are shown at $\times$20 (D) or $\times$63 (B and C) magnification. (E) Additionally, 5×10^5 differentiated VZV ORF63, CT, and UT SH-SY5Y cells were fixed, permeabilized, stained for HA, and analyzed via flow cytometry. All the data presented are representative of three biological replicates, except for IFA staining (B and C), which is representative of two biological replicates.

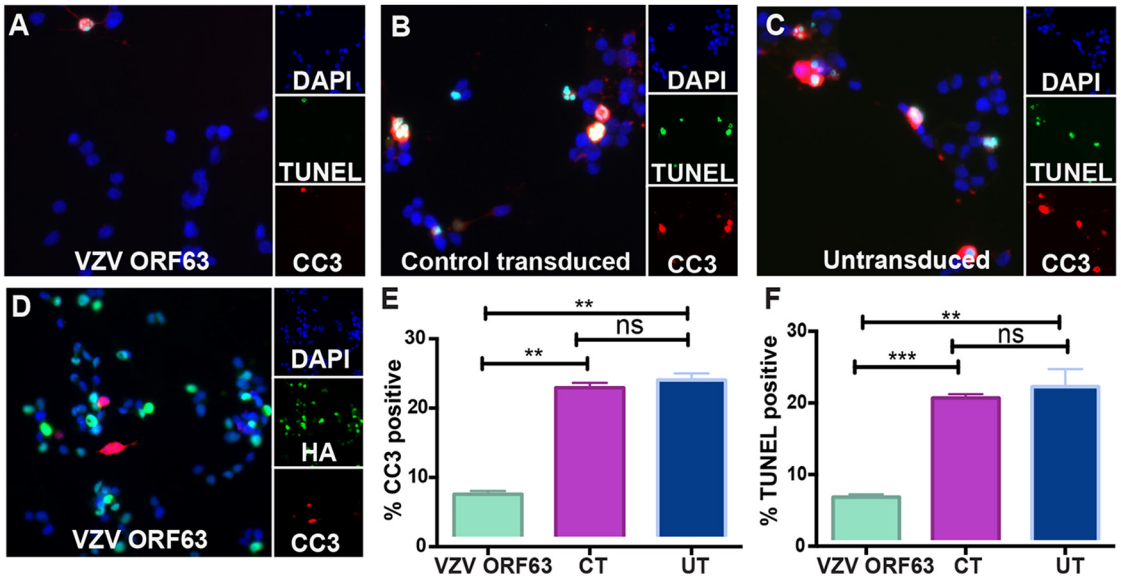

FIG 2 VZV ORF63 inhibits staurosporine-induced apoptosis in differentiated SH-SY5Y cells. (A to D) VZV ORF63 (A and D), CT (B), and UT (C) SH-SY5Y cells (1×10^5) were treated with ATRA for 5 days and differentiated on Matrigel-coated coverslips (13 mm; Knittel glass) via BDNF treatment. The cells were then treated with 0.5 μM staurosporine for 4 h to induce apoptosis and fixed with 4% paraformaldehyde. The cells were permeabilized and stained for CC3 (red) and TUNEL (green) (A to C) or HA (green) and CC3 (red) (D). (E) Cells were counterstained with nuclear DAPI (blue) and visualized by fluorescence microscopy. The images are shown at ×20 magnification and are representative of three biological replicates. (F) For cell counts, 10 different fields of view were imaged to calculate the percentage of CC3- or TUNEL-positive cells under each condition. (E and F) The error bars show standard errors of the mean (SEM), and statistical significance was established by Student's paired *t* test ns, not significant [$P \geq 0.05$]; **, $P < 0.01$; ***, $P < 0.005$.

experiments (Fig. 2E and F). We found that VZV ORF63 SH-SY5Y cells were significantly less TUNEL and CC3 positive than CT and UT cells (Fig. 2E and F). Additionally, no significant differences were found between CT and UT SH-SY5Y cells, suggesting transduction alone does not affect the ability of the cells to undergo apoptosis. To ascertain whether the HA-ORF63-expressing cells were protected from apoptosis, the cells were dually immunostained for HA and CC3 and assessed by fluorescence microscopy (Fig. 2D). No HA-ORF6-expressing cells were found to be CC3 positive. These data show that expression of VZV ORF63 alone is sufficient to inhibit staurosporine-induced apoptosis in differentiated human SH-SY5Y neuronal cells.

VZV rOka induces only a small degree of apoptosis in HaCaT cells. We have shown that VZV ORF63 can protect human neurons from apoptosis induction; however, it is unclear whether this phenotype can be observed in other clinically relevant cell types. Previously, our laboratory has shown that VZV-infected HFs are susceptible to apoptosis induction (22); however, other VZV genes, such as ORF12, have been shown to be protective in skin cells, such as MeWo cells (29). Keratinocytes have been shown to be infected in patient samples (40) and *in vitro* (41, 42). Interestingly, the ability of VZV to cause cell death in this cell type has not been fully characterized. We sought to characterize the ability of VZV strain rOka to induce apoptosis in HaCaT cells, a spontaneously immortalized human keratinocyte cell line (43). The HaCaT cell line has previously been shown to be infected with VZV (44) and thus was chosen as a suitable model for studying VZV proteins in keratinocytes.

VZV rOka-infected HaCaT cells or mock-infected HaCaT cells were stained with cell trace violet (CTV) and used to infect monolayers of HaCaT cells in a cell-associated manner at a 1:5 inoculum-to-cell ratio. CTV staining of the inoculating cells allowed the exclusion of the cells in subsequent flow cytometry analysis. VZV is highly cell associated *in vitro*, and therefore, cell-associated infections are standard practice to propagate infection; however, this results in asynchronous infection (45). Mock- and VZV-infected cells were collected at days 2, 3, and 5 postinfection (p.i.) for flow cytometry

detection of CC3 and LIVE/DEAD staining with Zombie NIR (Biolegend) (Fig. 3A). Both adherent and suspended cells were collected for flow cytometry analysis to ensure all dead cells were analyzed. VZV rOka-infected HaCaT cells were identified by VZV gEgI antigen (a late gene product) expression, and the cells were shown to be on average 20%, 28%, and 28% gEgI positive ($gEgI^+$) on days 2, 3, and 5, respectively, over three biological replicates (Fig. 4). Cells were classified as being live if they were Zombie NIR^- and $CC3^-$, as undergoing other cell death if they were Zombie NIR^+ and $CC3^-$, as undergoing late apoptosis if they were Zombie NIR^+ and $CC3^+$, and as undergoing early apoptosis if they were $CC3^+$ and Zombie NIR^- (Fig. 3A to E). Even by 5 days p.i., the VZV gEgI-positive cells had a percentage of live cells (measured by Zombie NIR staining) similar to those of both mock-infected and bystander gEgI-negative cells. In addition, results from 3 biological replicates showed that VZV gEgI-positive cells underwent significantly less other cell death at days 3 and 5 p.i. but slightly more early apoptosis at day 5 p.i. than both mock-infected and bystander gEgI-negative cells (Fig. 3B and E). However, for all other time points and types of cell death, VZV antigen-positive cells were comparable to mock-infected and gEgI-negative cells (Fig. 3B to E). To confirm that VZV rOka was not able to induce a large amount of apoptosis in the HaCaT cells, IFA analysis was conducted on rOka- and mock-infected HaCaT cells that were infected using the cell-associated method described above. Cells were collected each day for 3 days p.i. and stained for CC3, TUNEL, and VZV ORF40 (an early gene product) (Fig. 5). At all time points, there were similar levels of apoptotic cells among mock-infected and VZV rOka-infected cells, and the results were consistent in 3 biological repeats. Together, these results indicate that VZV rOka does not induce a large amount of apoptosis in HaCaT cells and suggest VZV gene products could delay virus-induced apoptosis.

Validation of VZV ORF63-expressing HaCaT cells. Our laboratory has previously suggested that the protective effect of ORF63 is neuron specific, as the loss of one of two copies of ORF63 from the virus resulted in an increase in apoptosis in neurons, but not in HFs (27). However, the ability of ORF63 alone to protect nonneuronal cell types from apoptosis has not been investigated. To study the protective effect of VZV ORF63 in a nonneuronal cell type, an HA-tagged VZV ORF63-expressing HaCaT cell line was generated via transduction with the VZV ORF63 pseudovirus (Fig. 6A and B). In parallel, a control pseudovirus was generated to create CT HaCaT cells. Immunostaining and microscopy revealed that the VZV ORF63 HaCaT cells expressed HA-tagged VZV ORF63 in both the nucleus and cytoplasm, which is consistent with the ORF63-expressing SH-SY5Y cells and previous reports (38) (Fig. 6A). On average, over three biological replicates, 50% of cells were determined to be HA positive after selection via flow cytometry (Fig. 6B). No specific HA staining was observed in control transduced or untransduced HaCaT cells by either method. Taking the data together, these HA-ORF63-expressing cell lines can be used to investigate the roles of ORF63 in a number of apoptosis pathways.

VZV ORF63 inhibits staurosporine- and FasL-induced apoptosis in HaCaT cells. Since VZV rOka induced minimal apoptosis in HaCaT cells, we sought to determine whether VZV ORF63 could protect against apoptosis in this cell type. Staurosporine and FasL were utilized to induce intrinsic and extrinsic apoptosis, respectively, to ascertain whether VZV ORF63 protection is specific to a particular type of apoptotic stimulus. VZV ORF63-expressing, CT, or UT HaCaT cells were treated with 0.5 μM staurosporine for 5 h and then stained for CC3 and TUNEL as described previously and visualized by fluorescence microscopy (Fig. 7A to C). Fewer CC3- and TUNEL-positive cells were observed in the VZV ORF63 HaCaT cells than in the CT and UT cells (Fig. 7A to C). To quantitate this difference, 10 independent fields of view for each cell type were enumerated for CC3- and TUNEL-positive cells (Fig. 7E and F). Significantly fewer VZV ORF63 HaCaT cells than CT and UT cells were CC3 positive and TUNEL positive (Fig. 7E and F). CT cells were not significantly different from UT cells, indicating that transduction alone does not affect the ability of the cell type to undergo apoptosis. Cells were

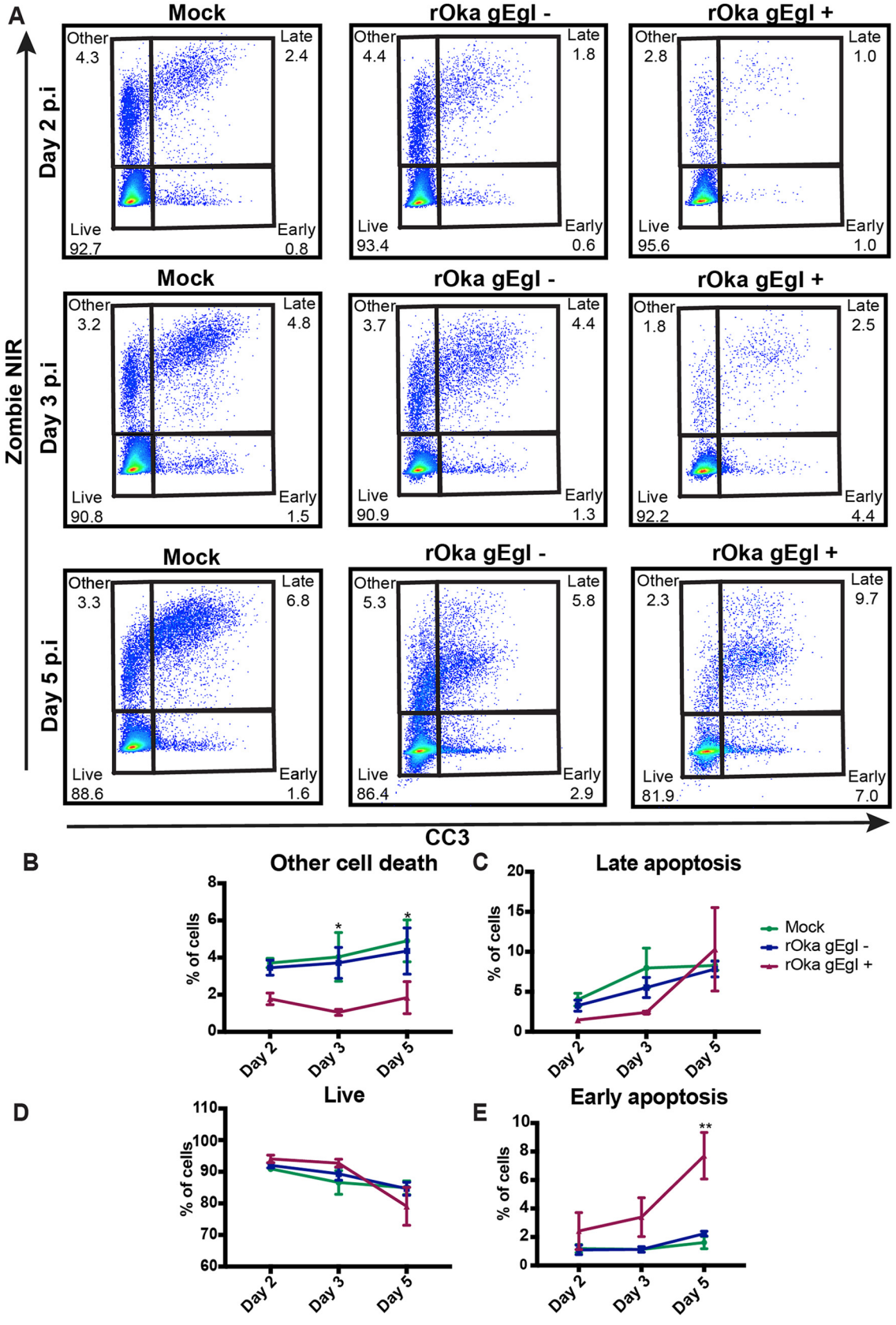

FIG 3 VZV rOka induces only a small degree of apoptosis in HaCaT cells. (A) HaCaT cells (5×10^5) were infected with either CTV-labeled VZV rOka inoculum or CTV-labeled mock inoculum at a ratio of 1:5 in a 6-well plate (Costar). Cells were collected at days 2, 3, and 5 p.i.; stained for VZV gEgI and CC3 and LIVE/DEAD stained to identify apoptotic cells; and analyzed by flow cytometry. The flow cytometry

(Continued on next page)

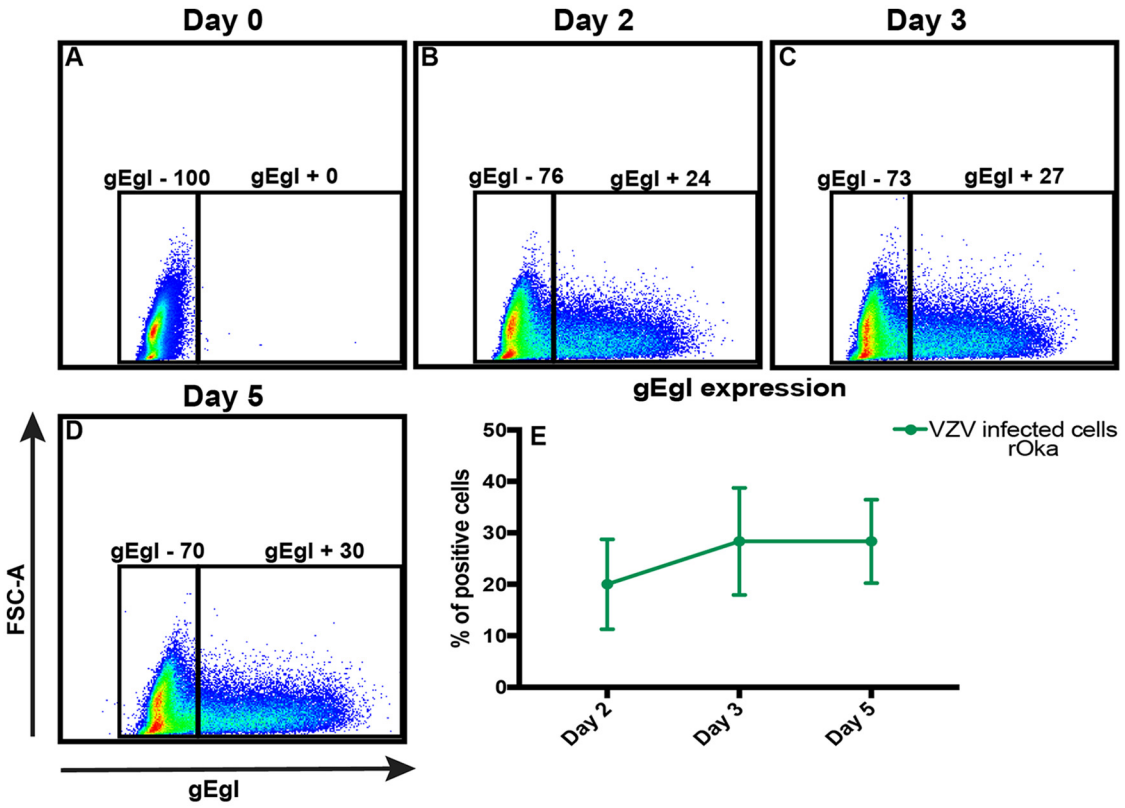

FIG 4 gEgI positivity of VZV rOka-infected HaCaT cells shown in Fig. 3. (A to D) HaCaT cells (5×10^5) were infected with either CTV-labeled VZV rOka inoculum or CTV-labeled mock inoculum at a ratio of 1:5 in a 6-well plate (Costar). Cells were collected at days 0, 2, 3, and 5 p.i.; stained for VZV gEgI and CC3 and LIVE/DEAD stained to identify apoptotic cells; and analyzed by flow cytometry. The flow cytometry plots are representative of three biological replicates. (E) Percentages of gEgI-positive HaCaT cells. The graphs are representative of the collation of three biological replicates. The error bars show SEM.

also dually immunostained for HA and CC3 (Fig. 7D), and the HA-ORF63-expressing cells were not CC3 positive.

For FasL-induced apoptosis, cells were treated with 100 ng/ml FasL for 4 h and immunostained for CC3 and TUNEL by fluorescence microscopy as previously described (Fig. 7G to L). The VZV ORF63 HaCaT cell population had significantly fewer CC3-positive cells than CT and UT HaCaT cells. There was minimal TUNEL staining in all three cell types (Fig. 7G to I). These differences were enumerated as described above, and it was clear that VZV ORF63-expressing cells were significantly less CC3 positive than CT and UT cells (Fig. 7K); however, this pattern was not discerned for TUNEL positivity, due to minimal TUNEL staining being observed (Fig. 7L). There were no significant differences between CT and UT cells. FasL-treated cells were also dually immunostained for CC3 and HA expression, and it was observed that VZV ORF63-expressing cells were not CC3 positive (Fig. 7J). Together, these data demonstrate that VZV ORF63 protects HaCaT cells from staurosporine- and FasL-induced apoptosis.

VZV ORF63 localization changes upon intrinsic apoptosis induction. It has become apparent that VZV ORF63 can protect both human HaCaT keratinocytes and differentiated human SH-SY5Y neuronal cells from apoptosis; however, it is still unclear how the protein modulates this effect. To begin to elucidate this, we sought to determine whether ORF63 localization changes during apoptosis induction. VZV ORF63

FIG 3 Legend (Continued)
plots are representative of three biological replicates. (B to E) Percentages of cells undergoing other cell death (B), late apoptosis (C), or early apoptosis (E) or that were alive (D) over the time course after infection. The graphs are representative of the collation of three biological replicates. The error bars show SEM. Statistical significance was established by a 2-way ANOVA using Tukey's multiple-comparison test. *, $P < 0.05$; **, $P < 0.01$.

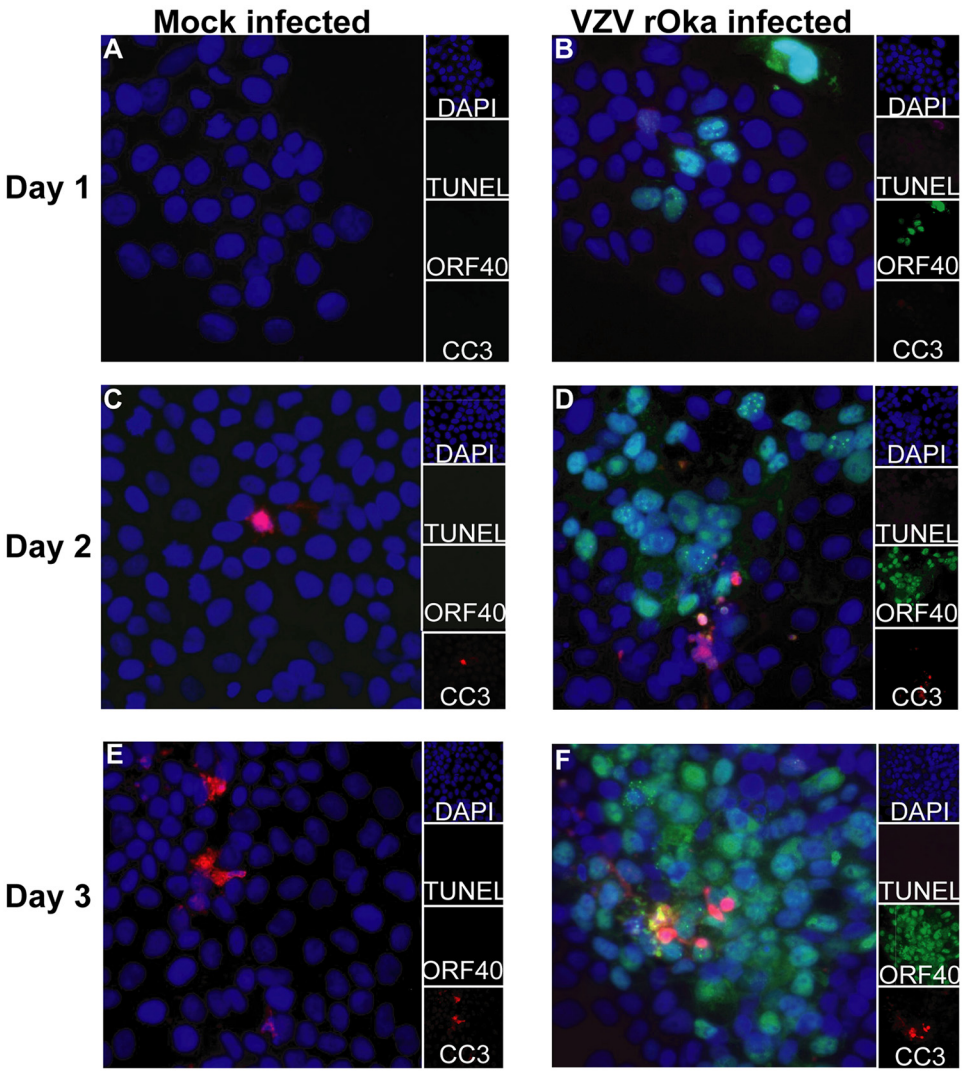

FIG 5 VZV rOka induces only a small degree of apoptosis over a 3-day time course measured by IFA. (A to F) HaCaT cells (1×10^5) were seeded onto coverslips (13 mm; Knittel glass) and infected with either VZV rOka inoculum or mock inoculum at a ratio of 1:5. Cells were collected at days 1, 2, and 3 p.i. and fixed with 4% paraformaldehyde. The cells were permeabilized and stained for CC3 (red) and VZV ORF40 (green) and TUNEL stained (magenta). The cells were counterstained with nuclear DAPI (blue) and were visualized by fluorescence microscopy. The images are shown at ×20 magnification and are representative of three biological replicates.

HaCaT cells treated with 0.5 μM staurosporine for 3 h (Fig. 8A) or untreated (Fig. 8B) were stained with MitoTracker deep red FM (Life Technologies), fixed, permeabilized, and immunostained for HA. Confocal microscopy revealed that VZV ORF63 expression became more cytoplasmic; additionally, there appeared to be formation of HA-positive aggregates.

To determine whether this change in localization was consistent with ORF63 protein expression during VZV infection, at day 3 p.i., VZV rOka-infected HaCaT cells were treated with 0.5 μM staurosporine (Fig. 8C and E) for 3 h or were left untreated (Fig. 8D and F). The cells were stained with MitoTracker deep red FM, fixed, permeabilized, and immunostained for VZV ORF63 or VZV ORF40. During VZV infection VZV ORF63 became markedly more cytoplasmic during apoptosis induction, and again, aggregate formation was identifiable (Fig. 8C and D). In contrast to this, ORF40 localization during apoptosis induction remained largely nuclear (Fig. 8E and F), suggesting that the phenotype observed for VZV ORF63 is a specific relocalization and not merely a consequence arising from cell stress associated with apoptosis. These data suggest that

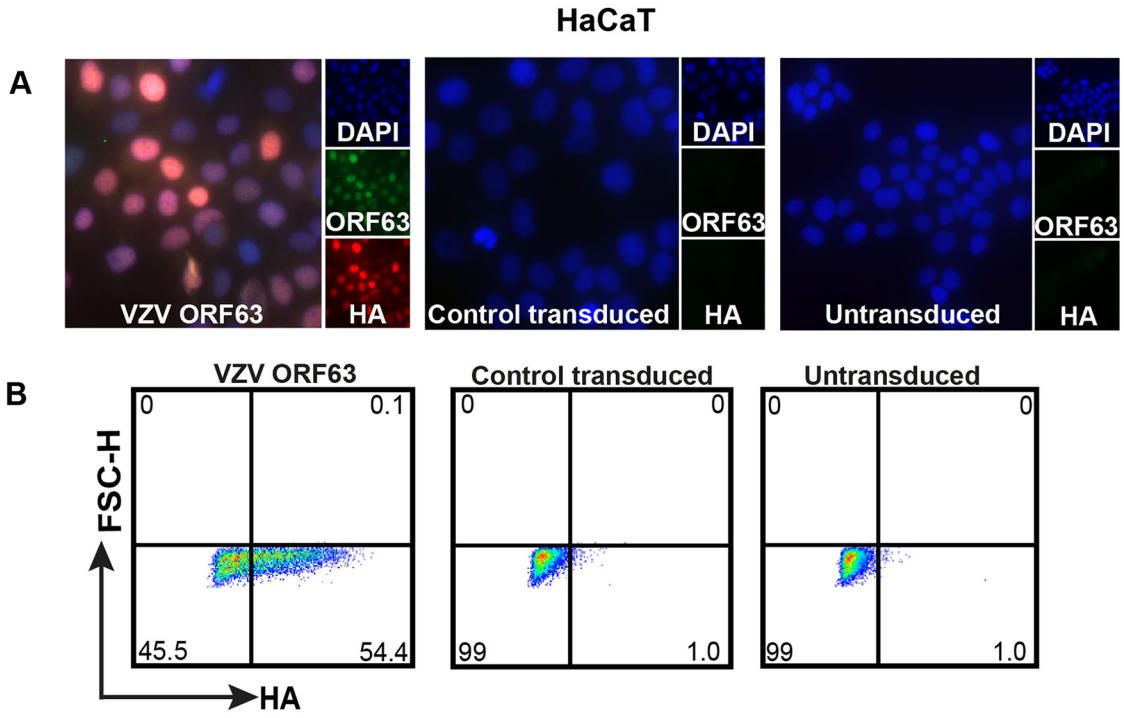

FIG 6 Validation of HA-tagged VZV ORF63-expressing HaCaT cells. (A) HaCaT cells (9×10^5) were transduced with VZV ORF63 or CT pseudoviruses and were selected with 0.5 mg/ml G418 for 10 days to create VZV ORF63, CT, and untransduced HaCaT cells. VZV ORF63, control transduced, and untransduced HaCaT cells (1×10^5) were seeded on coverslips (13 mm; Knittel glass), fixed with 4% PFA, and stained for HA (red) and VZV ORF63 (green). The cells were counterstained with nuclear DAPI (blue) and visualized by fluorescence microscopy. The images are shown at ×20 magnification. (B) Additionally, 5×10^5 VZV ORF63, CT, and UT HaCaT cells were fixed, permeabilized, stained for HA, and analyzed via flow cytometry. All the data presented are representative of three biological replicates.

VZV ORF63 relocalizes during apoptosis induction in human keratinocytes, implying a potential function for ORF63 in the cytoplasm.

DISCUSSION

The current study demonstrates that VZV ORF63 expressed in isolation in human neuronal cell and keratinocyte lines can protect against apoptosis induction. We also characterized the ability of VZV rOka to induce cell death in the human HaCaT keratinocyte line, observing that the virus delayed apoptosis induction over a 5-day time course. We began to elucidate the mechanism behind VZV ORF63 protection by demonstrating that VZV ORF63 protein changes its localization during apoptosis induction, suggesting interaction with proteins in the apoptotic pathway. These findings suggest that, due to its ability to modulate apoptosis in the skin and neuronal environments, VZV ORF63 may be a potential candidate for mutation to generate new attenuated VZV strains for use in vaccination (46).

VZV is a neurotropic virus that establishes lifelong latency in the DRG. As neurons are senescent, it is not surprising that the virus modulates apoptosis to ensure latency is maintained and that reactivation is successful. We have previously demonstrated that VZV ORF63 is associated with neuronal protection from apoptosis; however, there has been no direct evidence that VZV ORF63 expression alone can protect human neuronal cells from apoptosis. Through the construction of novel VZV ORF63-expressing SH-SY5Y cells, we have been able to dissect the protective phenotype of ORF63. We demonstrated that VZV ORF63 expression alone is enough to protect differentiated human SH-SY5Y neuronal cells from staurosporine-induced apoptosis, consolidating our previous work. It is important to note that differentiated SH-SY5Y cells have more properties of central neurons than of peripheral neurons (47, 48), and thus, it would be beneficial to repeat these experiments in primary human peripheral neurons. As VZV ORF63 is one of the most prominent transcripts produced in latency (32–34, 49), it is

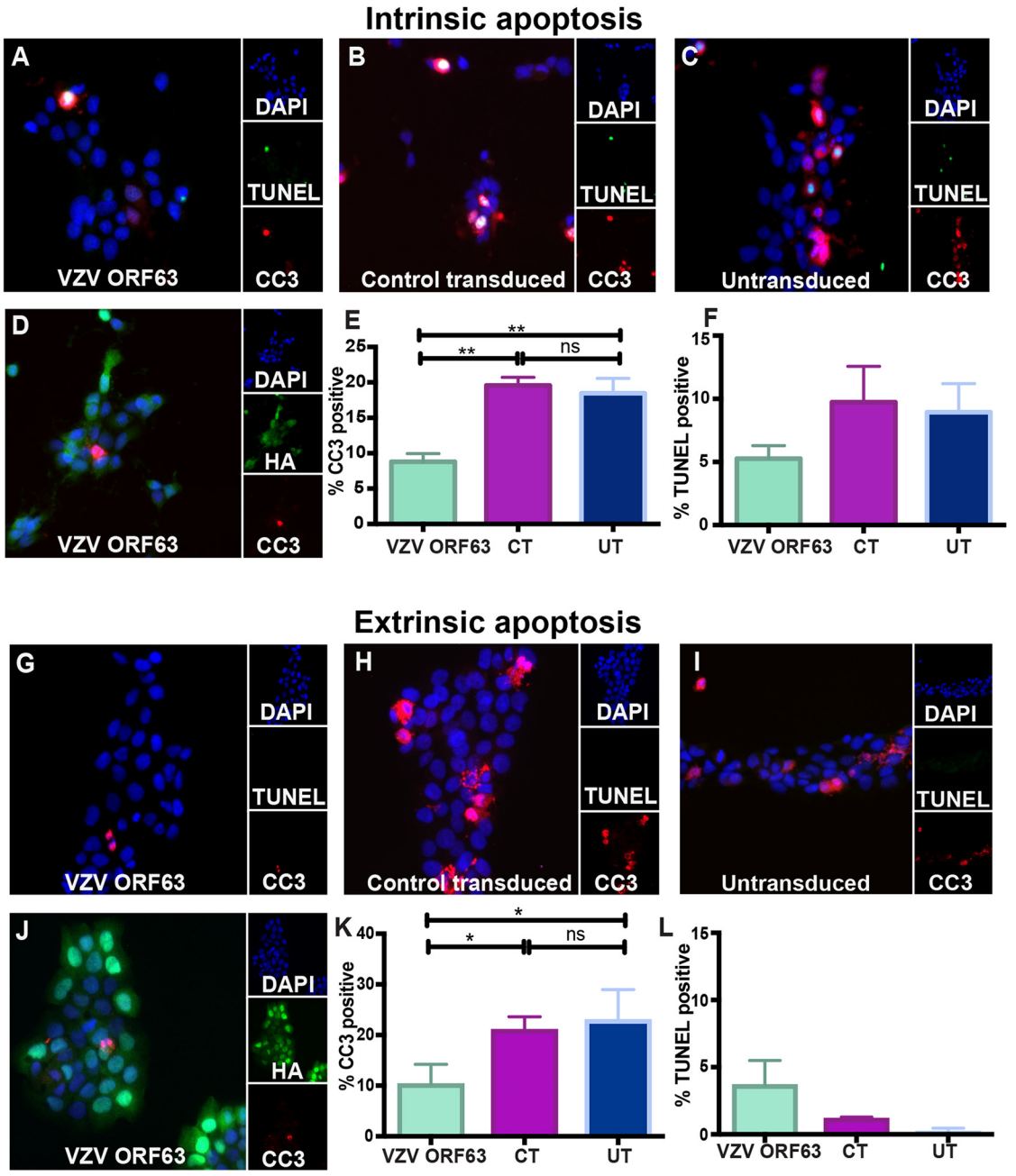

FIG 7 VZV ORF63 inhibits staurosporine- and FasL-induced apoptosis in HaCaT cells. VZV ORF63 (A, D, G, and J), CT (B and H), and UT (C and I) HaCaT cells (1×10^5) were treated with 0.5 μM staurosporine (A to F) or 100 ng FasL (G to L) for 5 h and fixed with 4% paraformaldehyde on coverslips (13 mm; Knittel glass). The cells were permeabilized and stained for CC3 (red) and TUNEL stained (green) (A to C and G to I) or stained for HA (green) and CC3 (red) (D and J). The cells were counterstained with nuclear DAPI (blue) and visualized by fluorescence microscopy. The images are shown at ×20 magnification and are representative of three biological replicates. For the cell counts, 10 different fields of view were imaged to calculate the percentage of CC3-positive (E and K) or TUNEL-positive (F and L) cells under each condition. The error bars show SEM, and statistical significance was established by Student's paired *t* test (ns, not significant [$P \geq 0.05$]; *, $P < 0.05$; **, $P < 0.01$).

conceivable that VZV ORF63's ability to inhibit apoptosis also enables the virus to establish latency, maintain latency, and reactivate.

Various studies have demonstrated that VZV induces apoptosis in cell types such as HFs (22), MeWo cells (23), and immune cells (e.g., T cells, B cells, and monocytes) (24, 25). The ability of VZV to induce or protect against cell death has not been fully characterized in keratinocytes. Sensory neurons of the DRG dock in the keratinocyte

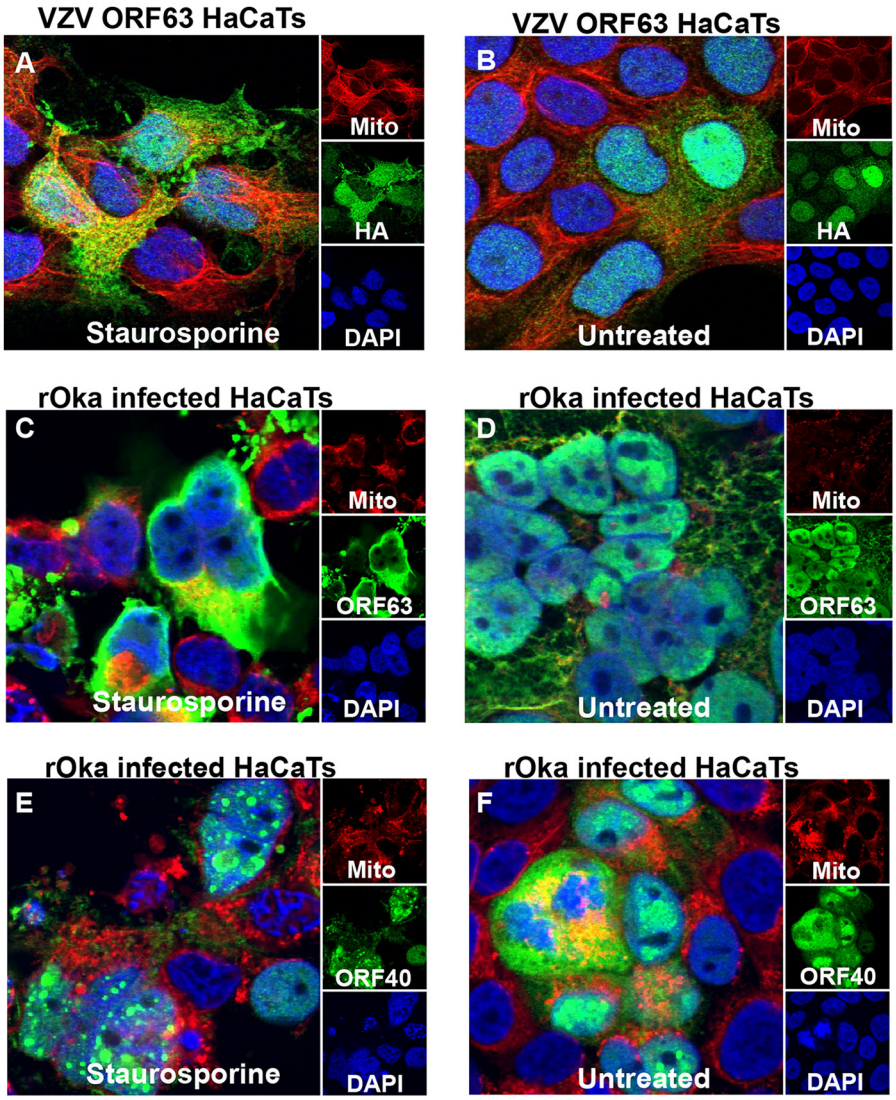

FIG 8 VZV ORF63 protein localization changes with staurosporine treatment. VZV ORF63-expressing HaCaT cells (A and B) and rOka-infected HaCaT cells (C to F) were treated with 0.5 μM staurosporine for 3 h (A, C, and E) or were left untreated (B, D, and F). The cells were stained with MitoTracker deep red (red); fixed with 4% paraformaldehyde; permeabilized; and stained for HA, VZV ORF40, or VZV ORF63 (green). The cells were counterstained with nuclear DAPI (blue) and visualized by fluorescence microscopy. The images are shown at $\times$63 magnification and are representative of three biological replicates.

layer of the epidermis (50), and therefore, modulation of cell death in keratinocytes could promote VZV infection of sensory neurons of the DRG. It is critical to explore the types of cell death induced by the virus due to their different inflammatory capacities, with apoptosis being noninflammatory and other forms of cell death, such as pyroptosis, necroptosis, and necrosis, being inflammatory (51). In the current study, we were able to distinguish between cells that were alive, in early apoptosis, in late apoptosis, or undergoing another form of cell death. Some reports in the literature suggest that HaCaT cells are capable of undergoing necroptosis (52, 53); however, in our and other's hands (E. Mocarski, Emory University, personal communication), using tumor necrosis factor (TNF) in combination with a second mitochondrion-derived activator of caspases (Smac) mimetic and pan-caspase inhibitor, HaCaT cells were not susceptible to necroptosis (Fig. 9). In the current study, we found that only a small percentage of human keratinocytes underwent early apoptosis up to 5 days p.i. with VZV rOka, indicating that the virus may delay apoptosis induction in these cells. Similar results were obtained by

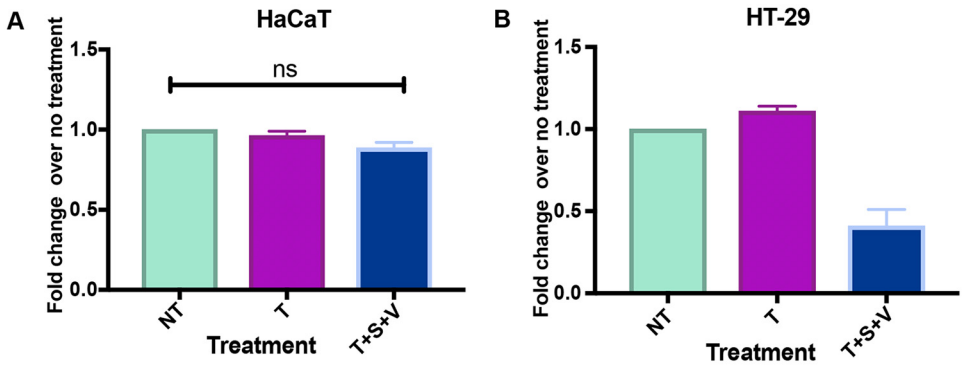

FIG 9 HaCaT cells cannot undergo necroptosis. HaCaT cells (3×10^4) (A) and HT-29 cells (2×10^4) (B) were seeded in triplicate in individual wells of a 96-well plate (Costar). To induce necroptosis (T+S+V), HT-29 cells and HaCaT cells were treated with 30 ng/ml TNF (T), 1 μM BV-6 (S), and 12.5 μM z-Vad (V) for 16 h. For the no-treatment control (NT), cells were treated with DMSO, and for the cell survival control (T), cells were treated with TNF alone. Cell viability was measured by CellTitre-Glo 2.0 assay using a Tecan plate reader. For HaCaT cells, three biological replicates were conducted; for HT-29 cells, two biological replicates were conducted. The error bars show SEM, and statistical significance was established by Student's paired *t* test (ns = not significant [$P \geq 0.05$]).

Black et al. (41), where VZV-infected human papillomavirus (HPV)-immortalized keratinocytes were negative for annexin V staining at 10 days p.i. Interestingly, VZV antigen-positive cells seemed to undergo less non-caspase 3-dependent cell death than mock-infected cells; therefore, it is prudent to explore the roles of different forms of cell death in the skin microenvironment.

Based on the observation that VZV delayed apoptosis induction in keratinocytes, we thought it would be interesting to explore the role of VZV ORF63 in that cell type. As a result, we constructed a novel VZV ORF63-expressing HaCaT cell line. VZV ORF63 was found to protect HaCaT cells from both staurosporine- and FasL-induced apoptosis, demonstrating that the protective effect provided by ORF63 is not exclusive to neurons or apoptotic stimuli. This is the first time that ORF63 has been shown to modulate FasL-induced extrinsic apoptosis. Confocal microscopy was utilized to examine VZV ORF63 protein localization during apoptosis induction, as it has been demonstrated that during infection, VZV ORF63 can localize to the mitochondria in human lung cells (54), which could be where VZV ORF63 modulates apoptosis. In both VZV-infected cells and VZV ORF63-expressing HaCaT cells, VZV ORF63 became more distinctly cytoplasmic upon apoptosis induction; however, localization to the mitochondria was not clear due to a diffuse ORF63 staining pattern. Interestingly, aggregate formation was also observed, indicating a potential protein-protein interaction. This change was shown not to be a by-product of cell death, as the same pattern was not observed with VZV ORF40, a protein with no known antiapoptotic functions.

It is important to elucidate the mechanism by which VZV gene products are able to protect against apoptosis, due to their importance in pathogenesis. VZV ORF63 is homologous to HSV ICP22, and both have been found to be antiapoptotic; however, there are key differences in their functions (55). HSV ICP22 produces a full-length ICP22 protein and an N-terminally truncated form called Us1.5 (56). Us1.5 acts to activate caspase 3 and thus induce apoptosis (57), while ICP22 has been suggested to antagonize p53 (58); however, it is not clear if this is responsible for ICP22 apoptosis inhibition (55). VZV ORF63 produces only a full-length protein, and unlike HSV ICP22, transcript and ORF63 protein are present during latency (34, 49). HSV encodes a latency-associated transcript known as LAT that has been shown to inhibit apoptosis by affecting apoptotic proteins, and also through the production of microRNAs that target apoptotic genes (55). VZV ORF63 is not known to encode any microRNAs or to transcriptionally regulate apoptotic proteins. Cell stress could activate the translation of the protein to inhibit apoptosis in latently infected neurons.

In summary, our results provide the first evidence that VZV ORF63 alone is enough

to protect differentiated human SH-SY5Y neuronal cells from apoptosis. Additionally, this is the first demonstration that VZV ORF63's protective effect is not neuron specific and can protect human HaCaT keratinocyte cells from both intrinsic and extrinsic apoptosis. This implicates VZV ORF63 as being crucial in VZV pathogenesis in the skin. We have begun to elucidate the mechanism of action of VZV ORF63 by showing that protein localization changes with apoptosis induction, suggesting protein-protein interactions with the apoptosis machinery. Altogether, our work helps to uncover the potential role of VZV ORF63 apoptosis modulation in VZV latency, reactivation, and ultimately pathogenesis.

MATERIALS AND METHODS

Cell lines. HEK293T cells (ATCC), HaCaT cells (Creative Bioarray), and HT-29 cells (ATCC) were maintained in Dulbecco's modified Eagle's medium (DMEM) supplemented with 10% fetal bovine serum (FBS) and 50 IU/ml penicillin and streptomycin.

SH-SY5Y neuroblastoma cells (ATCC) (59) were maintained in DMEM-F12 supplemented with 10% FBS and 50 IU/ml penicillin and streptomycin. To differentiate SH-SY5Y cells, the cells were treated with 10 μM ATRA for 5 days. Cells were then seeded onto Matrigel (Corning)-covered plates or flasks and treated with 50 ng/ml BDNF in serum-free medium for 4 days.

Viruses and infection of cell lines. VZV rOka (kindly provided by Ann Arvin, Stanford University) (60)-infected HaCaT cells were cocultivated with uninfected HaCaT cells at a 1:5 ratio.

HaCaT cells and undifferentiated SH-SY5Y cells were transduced with control or VZV ORF63 pseudoviruses, using 8 μg/ml of Polybrene. SH-SY5Y cells and HaCaT cells were selected with 0.4 mg/ml and 0.75 mg/ml G418, respectively, for 10 days. This generated VZV ORF63-expressing HaCaT cells, CT HaCaT cells, VZV ORF63-expressing SH-SY5Y cells, and CT SH-SY5Y cells. Undifferentiated ORF63-expressing SH-SY5Y and CT SH-SY5Y cells were differentiated before use in experiments.

Apoptosis and necroptosis treatments and cell viability measurement. To induce apoptosis, differentiated SH-SY5Y cells were treated with 0.5 μM staurosporine for 4 h and HaCaT cells were treated with 0.5 μM staurosporine for 5 h or with 100 ng/μl Fas ligand for 5 h. To induce necroptosis, HT-29 cells and HaCaT cells were treated with 30 ng/ml TNF, 1 μM BV-6 (Smac mimetic), and 12.5 μM z-Vad (pan caspase inhibitor) for 16 h, and cell viability was measured by CellTitre-Glo 2.0 assay (Promega, USA). For the no-treatment control, cells were treated with dimethyl sulfoxide (DMSO), and for the cell survival control, cells were treated with TNF alone.

Lentivirus construction, production, and infection. Primers (IE63_FHA_Eco, GGCGCAATAGAATTC TACCATGTACCCATACGATGTTCCAGATTACGCTTTTTGCACCTCACCGGC, and IE63_R_Bam, GGCCGAAGGAT CCCTACACGCCATGGGGGG) were utilized to amplify VZV ORF63 from the VZV pOka genome (Ann Arvin, Stanford University), to attach an HA tag to the N-terminal region of the protein, and to insert appropriate restriction enzyme (RE) cut sites. PCR products were purified (GE Healthcare; Illustra GFX PCR DNA and gel band kit) and digested with EcoRI-HF and BamHI-HF REs. The backbone plasmid (pCDH1-CMV-MCS-EF1-Neo cDNA cloning and expression vector [pCDH]; System Biosciences, USA) was also digested with EcoRI-HF and BamHI-HF and ligated with the VZV ORF63 PCR product using T4 DNA ligase (NEB); the resulting plasmid was called pCDH63. pCDH63 was transformed into *Escherichia coli* Stbl2 competent cells (NEB) and collected using a plasmid DNA purification kit (Nucleobond Xtra Midi plasmid DNA purification kit; Macherey-Nagel). pCDH63 was transfected into 293T cells with the packaging plasmids psPAX2 (Addgene) and pMD2G (Addgene) using Fugene HD (Promega) to create an HA-VZV ORF63-expressing pseudovirus. pCDH was transfected into 293T cells with the packaging plasmids psPAX2 and pMD2G using Fugene HD to create the corresponding control pseudovirus.

Flow cytometry. Mock-infected or VZV rOka-infected HaCaT cells were stained with 1 μl/ml CTV (Thermo Fisher Scientific) for 20 min at 37°C. The cells were then quenched in medium and seeded onto uninfected HaCaT cells at a ratio of 1:5. At days 2, 3, and 5 p.i., cells were collected for flow cytometry. The cells were stained with Zombie NIR and rabbit anti-VZV gEgI (Meridian Bioscience Inc.) that was conjugated to Dylight 488 (Serotec) at room temperature (RT) for 30 min protected from light and were then fixed and permeabilized (BD Fix Perm) at 4°C. The cells were stained with rabbit anti-CC3-phycoerythrin (PE) (BD Biosciences) overnight at 4°C. All samples were acquired on an LSR Fortessa flow cytometer (BD Biosciences) and analyzed with FloJo software (Tree Star, Ashland, OR). CTV-labeled inoculum cells were excluded from the analysis.

TUNEL assay and MitoTracker staining. Cells were grown on coverslips and treated as indicated. The cells were washed with phosphate-buffered saline (PBS) and fixed with 4% paraformaldehyde (PFA) for 15 min at RT. After washing with PBS, the cells were permeabilized with 0.1% Triton X (Sigma-Aldrich) for 10 min and blocked using 20% normal donkey serum (NDS) (Sigma-Aldrich). The cells were TUNEL stained (In Situ Cell Death Detection kit, fluorescein; Roche) for 1 h at 37°C.

For MitoTracker deep red FM staining, cells were stained with 0.3 μM MitoTracker deep red FM for 30 min at 37°C and washed with PBS. The cells were fixed with 4% PFA for 15 min at RT.

IFA. Cells were grown on coverslips and treated/infected as indicated. The cells were washed with PBS and fixed with 4% PFA for 15 min at RT. After washing with PBS, the cells were permeabilized with 0.1% Triton X (Sigma-Aldrich) for 10 min and blocked using 20% NDS (Sigma-Aldrich). The cells were incubated with primary antibodies or corresponding isotype controls for 1 h at RT. The cells were washed with PBS, incubated with secondary antibodies at RT for 30 min, and washed with PBS, and coverslips were mounted on glass slides using Prolong Gold Anti-Fade reagent with DAPI (4′,6-diamidino-2-

phenylindole) (Life Technologies). Staining was visualized on a Zeiss Axio Imager microscope or Zeiss LSM 510 Meta Spectral confocal microscope, and images were taken using Zen software (Zeiss) or LSM 510 (Zeiss), respectively. Images were pseudocolored using Fiji (Image J). For apoptosis quantification, 10 independent images of each coverslip were taken, and CC3- and TUNEL-positive cells were counted manually to calculate an average percentage of positive cells.

Antibodies. For IFA, cells were stained with the following primary antibodies as indicated: mouse anti-VZV ORF40 (NCP-1; 1:500; Meridian Bioscience Inc.), mouse anti-HA tag (6E2; 1:100; Cell Signaling Technology), rabbit anti-CC3 (D3E9; 1:150; Cell Signaling Technology), mouse anti-NCAM (123C3; 1:20; Cell Signaling Technology), rabbit anti-synaptophysin (Z66; 1:10; Invitrogen), and rabbit anti-VZV ORF63 (1:300; a gift from Paul Kinchington, University of Pittsburgh).

For IFA, cells were stained with the following secondary antibodies (1:250; Invitrogen) as indicated: donkey anti-rabbit IgG 488, 594, and 647 and donkey anti-mouse IgG 488, 546, 594, and 647.

Statistical analysis. *P* values were determined for IFA analysis using a paired 2-tailed Student *t* test. *P* values were determined for flow cytometry analysis via a 2-way analysis of variance (ANOVA) using Tukey's multiple-comparison test.

ACKNOWLEDGMENTS

Chelsea Gerada was supported by an Australian Postgraduate Award.

We acknowledge the assistance of Louise Cole of the Bosch Institute Advanced Microscopy Facility, University of Sydney, and the flow cytometry core of Sydney Cytometry.

REFERENCES

1. Zerboni L, Sen N, Oliver SL, Arvin AM. 2014. Molecular mechanisms of varicella zoster virus pathogenesis. Nat Rev Microbiol 12:197–210. https://doi.org/10.1038/nrmicro3215.
2. Watson CPN, Evans RJ, Watt VR, Birkett N. 1988. Post-herpetic neuralgia: 208 cases. Pain 35:289–297. https://doi.org/10.1016/0304-3959(88)90139-X.
3. James SF, Mahalingam R, Gilden D. 2012. Does apoptosis play a role in varicella zoster virus latency and reactivation? Viruses 4:1509–1514. https://doi.org/10.3390/v4091509.
4. Elmore S. 2007. Apoptosis: a review of programmed cell death. Toxicol Pathol 35:495–516. https://doi.org/10.1080/01926230701320337.
5. Westphal D, Kluck R, Dewson G. 2014. Building blocks of the apoptotic pore: how Bax and Bak are activated and oligomerize during apoptosis. Cell Death Differ 21:196–205. https://doi.org/10.1038/cdd.2013.139.
6. Kluck RM, Degli Esposti M, Perkins G, Renken C, Kuwana T, Bossy-Wetzel E, Goldberg M, Allen T, Barber MJ, Green DR. 1999. The pro-apoptotic proteins, Bid and Bax, cause a limited permeabilization of the mitochondrial outer membrane that is enhanced by cytosol. J Cell Biol 147:809–822. https://doi.org/10.1083/jcb.147.4.809.
7. Desagher S, Osen-Sand A, Nichols A, Eskes R, Montessuit S, Lauper S, Maundrell K, Antonsson B, Martinou J-C. 1999. Bid-induced conformational change of Bax is responsible for mitochondrial cytochrome c release during apoptosis. J Cell Biol 144:891–901. https://doi.org/10.1083/jcb.144.5.891.
8. Zou H, Li Y, Liu X, Wang X. 1999. An APAF-1· cytochrome c multimeric complex is a functional apoptosome that activates procaspase-9. J Biol Chem 274:11549–11556. https://doi.org/10.1074/jbc.274.17.11549.
9. Cheng EH-Y, Wei MC, Weiler S, Flavell RA, Mak TW, Lindsten T, Korsmeyer SJ. 2001. BCL-2, BCL-X(L) sequester BH3 domain-only molecules preventing BAX-and BAK-mediated mitochondrial apoptosis. Molecular Cell 8:705–711. https://doi.org/10.1016/S1097-2765(01)00320-3.
10. Czabotar PE, Lessene G, Strasser A, Adams JM. 2014. Control of apoptosis by the BCL-2 protein family: implications for physiology and therapy. Nat Rev Mol Cell Biol 15:49–63. https://doi.org/10.1038/nrm3722.
11. Pop C, Salvesen GS. 2009. Human caspases: activation, specificity, and regulation. J Biol Chem 284:21777–21781. https://doi.org/10.1074/jbc.R800084200.
12. Kischkel F, Hellbardt S, Behrmann I, Germer M, Pawlita M, Krammer P, Peter M. 1995. Cytotoxicity-dependent APO-1 (Fas/CD95)-associated proteins form a death-inducing signaling complex (DISC) with the receptor. EMBO J 14:5579.
13. Li H, Zhu H, Xu C-J, Yuan J. 1998. Cleavage of BID by caspase 8 mediates the mitochondrial damage in the Fas pathway of apoptosis. Cell 94:491–501. https://doi.org/10.1016/S0092-8674(00)81590-1.
14. Roulston A, Marcellus RC, Branton PE. 1999. Viruses and apoptosis. Annu Rev Microbiol 53:577–628. https://doi.org/10.1146/annurev.micro.53.1.577.
15. Lagunoff M, Carroll PA. 2003. Inhibition of apoptosis by the γ-herpesviruses. Int Rev Immunol 22:373–399. https://doi.org/10.1080/08830180305218.
16. Henderson S, Huen D, Rowe M, Dawson C, Johnson G, Rickinson A. 1993. Epstein-Barr virus-coded BHRF1 protein, a viral homologue of Bcl-2, protects human B cells from programmed cell death. Proc Natl Acad Sci U S A 90:8479–8483. https://doi.org/10.1073/pnas.90.18.8479.
17. Norris KL, Youle RJ. 2008. Cytomegalovirus proteins vMIA and m38. 5 link mitochondrial morphogenesis to Bcl-2 family proteins. J Virol 82:6232–6243. https://doi.org/10.1128/JVI.02710-07.
18. Arnoult D, Bartle LM, Skaletskaya A, Poncet D, Zamzami N, Park PU, Sharpe J, Youle RJ, Goldmacher VS. 2004. Cytomegalovirus cell death suppressor vMIA blocks Bax- but not Bak-mediated apoptosis by binding and sequestering Bax at mitochondria. Proc Natl Acad Sci U S A 101:7988–7993. https://doi.org/10.1073/pnas.0401897101.
19. Cam M, Handke W, Picard-Maureau M, Brune W. 2010. Cytomegaloviruses inhibit Bak- and Bax-mediated apoptosis with two separate viral proteins. Cell Death Differ 17:655–665. https://doi.org/10.1038/cdd.2009.147.
20. Benetti L, Munger J, Roizman B. 2003. The herpes simplex virus 1 US3 protein kinase blocks caspase-dependent double cleavage and activation of the proapoptotic protein BAD. J Virol 77:6567–6573. https://doi.org/10.1128/JVI.77.11.6567-6573.2003.
21. Carpenter D, Hsiang C, Jiang X, Osorio N, BenMohamed L, Jones C, Wechsler SL. 2015. The herpes simplex virus type 1 (HSV-1) latency-associated transcript (LAT) protects cells against cold-shock-induced apoptosis by maintaining phosphorylation of protein kinase B (AKT). J Neurovirol 21:568–575. https://doi.org/10.1007/s13365-015-0361-z.
22. Hood C, Cunningham A, Slobedman B, Boadle R, Abendroth A. 2003. Varicella-zoster virus-infected human sensory neurons are resistant to apoptosis, yet human foreskin fibroblasts are susceptible: evidence for a cell-type-specific apoptotic response. J Virol 77:12852–12864. https://doi.org/10.1128/JVI.77.23.12852-12864.2003.
23. Brazeau E, Mahalingam R, Gilden D, Wellish M, Kaufer BB, Osterrieder N, Pugazhenthi S. 2010. Varicella-zoster virus–induced apoptosis in MeWo cells cells is accompanied by down-regulation of Bcl-2 expression. J Neurovirol 16:133–140. https://doi.org/10.3109/13550281003682547.
24. Koenig A, Wolff MH. 2003. Infectibility of separated peripheral blood mononuclear cell subpopulations by varicella-zoster virus (VZV). J Med Virol 70(Suppl 1):S59–S63. https://doi.org/10.1002/jmv.10323.
25. König A, Hömme C, Hauröder B, Dietrich A, Wolff MH. 2003. The varicella-zoster virus induces apoptosis in vitro in subpopulations of primary human peripheral blood mononuclear cells. Microbes Infect 5:879–889. https://doi.org/10.1016/S1286-4579(03)00177-1.
26. Sadzot-Delvaux C, Thonard P, Schoonbroodt S, Piette J, Rentier B. 1995.

Varicella-zoster virus induces apoptosis in cell culture. J Gen Virol 76:2875–2879. https://doi.org/10.1099/0022-1317-76-11-2875.
27. Hood C, Cunningham AL, Slobedman B, Arvin AM, Sommer MH, Kinchington PR, Abendroth A. 2006. Varicella-zoster virus ORF63 inhibits apoptosis of primary human neurons. J Virol 80:1025–1031. https://doi.org/10.1128/JVI.80.2.1025-1031.2006.
28. Schaap-Nutt A, Sommer M, Che X, Zerboni L, Arvin AM. 2006. ORF66 protein kinase function is required for T-cell tropism of varicella-zoster virus in vivo. J Virol 80:11806–11816. https://doi.org/10.1128/JVI.00466-06.
29. Liu X, Li Q, Dowdell K, Fischer ER, Cohen JI. 2012. Varicella-zoster virus ORF12 protein triggers phosphorylation of ERK1/2 and inhibits apoptosis. J Virol 86:3143–3151. https://doi.org/10.1128/JVI.06923-11.
30. Liu X, Cohen JI. 2013. Varicella-zoster virus ORF12 protein activates the phosphatidylinositol 3-kinase/Akt pathway to regulate cell cycle progression. J Virol 87:1842–1848. https://doi.org/10.1128/JVI.02395-12.
31. Liu X, Cohen JI. 2014. Inhibition of Bim enhances replication of varicella-zoster virus and delays plaque formation in virus-infected cells. J Virol 88:1381–1388. https://doi.org/10.1128/JVI.01695-13.
32. Cohen JI, Cox E, Pesnicak L, Srinivas S, Krogmann T. 2004. The varicella-zoster virus open reading frame 63 latency-associated protein is critical for establishment of latency. J Virol 78:11833–11840. https://doi.org/10.1128/JVI.78.21.11833-11840.2004.
33. Cohen JI, Krogmann T, Bontems S, Sadzot-Delvaux C, Pesnicak L. 2005. Regions of the varicella-zoster virus open reading frame 63 latency-associated protein important for replication in vitro are also critical for efficient establishment of latency. J Virol 79:5069–5077. https://doi.org/10.1128/JVI.79.8.5069-5077.2005.
34. Debrus S, Sadzot-Delvaux C, Nikkels AF, Piette J, Rentier B. 1995. Varicella-zoster virus gene 63 encodes an immediate-early protein that is abundantly expressed during latency. J Virol 69:3240–3245.
35. Tong H, Lu C, Wang L, Wang Q, Zhang J. 2010. Role of caspase-8 in TRAIL-induced apoptosis of neuroblastoma cell lines. Zhongguo Dang Dai Er Ke Za Zhi 12:902–907.
36. Christensen J, Steain M, Slobedman B, Abendroth A. 2011. Differentiated neuroblastoma cells provide a highly efficient model for studies of productive varicella-zoster virus infection of neuronal cells. J Virol 85:8436–8442. https://doi.org/10.1128/JVI.00515-11.
37. Encinas M, Iglesias M, Liu Y, Wang H, Muhaisen A, Cena V, Gallego C, Comella JX. 2000. Sequential treatment of SH-SY5Y cells with retinoic acid and brain-derived neurotrophic factor gives rise to fully differentiated, neurotrophic factor-dependent, human neuron-like cells. J Neurochem 75:991–1003. https://doi.org/10.1046/j.1471-4159.2000.0750991.x.
38. Bontems S, Di Valentin E, Baudoux L, Rentier B, Sadzot-Delvaux C, Piette J. 2002. Phosphorylation of varicella-zoster virus IE63 protein by casein kinases influences its cellular localization and gene regulation activity. J Biol Chem 277:21050–21060. https://doi.org/10.1074/jbc.M111872200.
39. Sato S, Fujita N, Tsuruo T. 2002. Interference with PDK1-Akt survival signaling pathway by UCN-01 (7-hydroxystaurosporine). Oncogene 21:1727–1738. https://doi.org/10.1038/sj.onc.1205225.
40. Nikkels AF, Rentier B, Piérard GE. 1997. Chronic varicella-zoster virus skin lesions in patients with human immunodeficiency virus are related to decreased expression of gE and gB. J Infect Dis 176:261–264. https://doi.org/10.1086/517262.
41. Black A, Jones L, Malavige G, Ogg G. 2009. Immune evasion during varicella zoster virus infection of keratinocytes. Clin Exp Dermatol 34:e941–e944. https://doi.org/10.1111/j.1365-2230.2009.03350.x.
42. Jones M, Dry IR, Frampton D, Singh M, Kanda RK, Yee MB, Kellam P, Hollinshead M, Kinchington PR, O'Toole EA. 2014. RNA-seq analysis of host and viral gene expression highlights interaction between varicella zoster virus and keratinocyte differentiation. PLoS Pathog 10:e1003896. https://doi.org/10.1371/journal.ppat.1003896.
43. Boukamp P, Petrussevska RT, Breitkreutz D, Hornung J, Markham A, Fusenig NE. 1988. Normal keratinization in a spontaneously immortalized aneuploid human keratinocyte cell line. J Cell Biol 106:761–771. https://doi.org/10.1083/jcb.106.3.761.
44. Crack L, Jones L, Malavige G, Patel V, Ogg G. 2012. Human antimicrobial peptides LL-37 and human β-defensin-2 reduce viral replication in keratinocytes infected with varicella zoster virus. Clin Exp Dermatol 37:534–543. https://doi.org/10.1111/j.1365-2230.2012.04305.x.
45. Weller TH. 1953. Serial propagation in vitro of agents producing inclusion bodies derived from varicella and herpes zoster. Exp Biol Med 83:340–346. https://doi.org/10.3181/00379727-83-20354.
46. Sadzot-Delvaux C, Rentier B. 2001. The role of varicella zoster virus immediate-early proteins in latency and their potential use as components of vaccines. Arch Virol Suppl 17:81–89.
47. Korecka JA, van Kesteren RE, Blaas E, Spitzer SO, Kamstra JH, Smit AB, Swaab DF, Verhaagen J, Bossers K. 2013. Phenotypic characterization of retinoic acid differentiated SH-SY5Y cells by transcriptional profiling. PLoS One 8:e63862. https://doi.org/10.1371/journal.pone.0063862.
48. Xie H-R, Hu L-S, Li G-Y. 2010. SH-SY5Y human neuroblastoma cell line: in vitro cell model of dopaminergic neurons in Parkinson's disease. Chin Med J 123:1086–1092.
49. Zerboni L, Sobel RA, Ramachandran V, Rajamani J, Ruyechan W, Abendroth A, Arvin A. 2010. Expression of varicella-zoster virus immediate-early regulatory protein IE63 in neurons of latently infected human sensory ganglia. J Virol 84:3421–3430. https://doi.org/10.1128/JVI.02416-09.
50. Keppel Hesselink JM, Kopsky DJ, Bhaskar AK. 2017. Skin matters! The role of keratinocytes in nociception: a rational argument for the development of topical analgesics. J Pain Res 10:1–6. https://doi.org/10.2147/JPR.S122765.
51. Kang R, Tang D. 2016. What is the pathobiology of inflammation to cell death? Apoptosis, necrosis, necroptosis, autophagic cell death, pyroptosis, and NETosis, p 81–106, In Maiuri MC, De Stefano D (ed), Autophagy networks in inflammation. Springer, Geneva, Switzerland.
52. Karl I, Jossberger-Werner M, Schmidt N, Horn S, Goebeler M, Leverkus M, Wajant H, Giner T. 2014. TRAF2 inhibits TRAIL-and CD95L-induced apoptosis and necroptosis. Cell Death Dis 5:e1444. https://doi.org/10.1038/cddis.2014.404.
53. Zhang W-J, Song Z-B, Bao Y-L, Li W-L, Yang X-G, Wang Q, Yu C-L, Sun L-G, Huang Y-X, Li Y-X. 2016. Periplogenin induces necroptotic cell death through oxidative stress in HaCaT cells and ameliorates skin lesions in the TPA-and IMQ-induced psoriasis-like mouse models. Biochem Pharmacol 105:66–79. https://doi.org/10.1016/j.bcp.2016.02.001.
54. Keller AC, Badani H, McClatchey PM, Baird NL, Bowlin JL, Bouchard R, Perng G-C, Reusch JE, Kaufer BB, Gilden D. 2016. Varicella zoster virus infection of human fetal lung cells alters mitochondrial morphology. J Neurovirol 22:674–682. https://doi.org/10.1007/s13365-016-0457-0.
55. You Y, Cheng A-C, Wang M-S, Jia R-Y, Sun K-F, Yang Q, Wu Y, Zhu D, Chen S, Liu M-F. 2017. The suppression of apoptosis by α-herpesvirus. Cell Death Dis 8:e2749. https://doi.org/10.1038/cddis.2017.139.
56. Bowman JJ, Schaffer PA. 2009. Origin of expression of the herpes simplex virus type 1 protein US1.5. J Virol 83:9183–9194. https://doi.org/10.1128/JVI.00984-09.
57. Hagglund R, Munger J, Poon AP, Roizman B. 2002. US3 protein kinase of herpes simplex virus 1 blocks caspase 3 activation induced by the products of US1.5 and UL13 genes and modulates expression of transduced US1.5 open reading frame in a cell type-specific manner. J Virol 76:743–754. https://doi.org/10.1128/JVI.76.2.743-754.2002.
58. Maruzuru Y, Fujii H, Oyama M, Kozuka-Hata H, Kato A, Kawaguchi Y. 2013. Roles of p53 in herpes simplex virus 1 replication. J Virol 87:9323–9332. https://doi.org/10.1128/JVI.01581-13.
59. Biedler JL, Helson L, Spengler BA. 1973. Morphology and growth, tumorigenicity, and cytogenetics of human neuroblastoma cells in continuous culture. Cancer Res 33:2643–2652.
60. Cohen JI, Seidel KE. 1993. Generation of varicella-zoster virus (VZV) and viral mutants from cosmid DNAs: VZV thymidylate synthetase is not essential for replication in vitro. Proc Natl Acad Sci U S A 90:7376–7380. https://doi.org/10.1073/pnas.90.15.7376.